18th Brazilian Congress of Thermal Sciences and Engineering
November 16-20, 2020 (Online)

ENC-2020-0229
THERMAL ANALYSIS OF A HEAT PUMP SOLAR EVAPORATOR

Hélio Augusto Goulart Diniz
Federal University of Minas Gerais (UFMG), Post-Graduate Program in Mechanical Engineering, Av. Antonio Carlos, 6627 – Pampulha, Belo Horizonte - MG, 31270-901, Brazil
Federal University of Minas Gerais (UFMG), Department of Mechanical Engineering, Av. Antonio Carlos, 6627 – Pampulha, Belo Horizonte - MG, 31270-901, Brazil
University Center Estácio de Sá, Av. Francisco Sales, 23 – Floresta, Belo Horizonte - MG, 30150-220, Brazil
Faculty of Education of Minas Gerais (FACEMG)/ Belo Horizonte Institute of Higher Education (IBHES), Av. Vilarinho, 2395 – Venda Nova, Belo Horizonte - MG, 31615-250, Brazil
heliomecanica@ufmg.br

Stella Marys Silva Pinheiro
Federal University of Minas Gerais (UFMG), Post-Graduate Program in Mechanical Engineering, Av. Antonio Carlos, 6627 – Pampulha, Belo Horizonte - MG, 31270-901, Brazil
stella_marys_@hotmail.com

Andréa Oliveira Souza da Costa
Luiz Machado
Raphael Nunes de Oliveira
Federal University of Minas Gerais (UFMG), Post-Graduate Program in Mechanical Engineering, Av. Antonio Carlos, 6627 – Pampulha, Belo Horizonte - MG, 31270-901, Brazil
andreacosta@deq.ufmg.br, luizm@demec.ufmg.br, rphnunes@demec.ufmg.br

Abstract. The use of Heat Pump for heating residential water is a better energy solution than the electric shower. It is a system that saves electrical energy and when it is assisted by solar energy its efficiency becomes even higher. However, on cloudy or rainy days, the energy availability of the environment decreases, affecting the system performance. The objective of this work is to present a theoretical and experimental thermal analysis of a solar evaporator of an air-water heat pump prototype using R134a as refrigerant and operating in a situation with zero solar radiation. A deep energetic analysis of the solar evaporator was carried out regarding the contribution of several energy sources in the environment. Contributions by ambient radiation, sensitive heat and latent heat of the air were analyzed, and their participation in the thermal contribution of the evaporator was determined. The contribution of the latent heat rate of the air in relation to the total rate exchanged with the evaporator was 24%.

Keywords: Heat pump, water heating, solar evaporator, R134a.

1. INTRODUCTION

The heating of residential water in Brazil is traditionally done through the use of electric shower. According to the study of energy efficiency and distributed generation for the years 2014 to 2024, 16.1% of the electric energy consumption of households in Brazil in 2014 came from the use of this equipment. In 2015, this percentage dropped a little, going to 16.0%. The trend is to decrease in the coming years and the percentage may reach 14.5% in 2019 and 12.2% in 2024 (EPE, 2016a). There is a perspective of evolution in the percent of houses with water heating by solar heater until 2024, showing the evolution of this type of energy in Brazilian residential scenario. In view of the rising cost of electric energy production and growing consumption due to the increase of the population, it is important that researches in the area of energy efficiency are developed in search of alternatives for more efficient equipment (EPE, 2016b). A limitation on the use of a solar collector system to heat water is the deficit of solar energy on some days of the year (rainy or cloudy weather), making the process of water heating impossible. Due to this aspect, it becomes necessary the use of a solar collector with an auxiliary system for the days of low solar incidence.

One of the most promising technologies for the replacement of the electric shower when it comes to residential water heating is the use of the Heat Pump. A Heat Pump can work alone providing savings in electricity consumption in relation to the shower or can work as auxiliary equipment in a solar collector system (Rodríguez et al., 2015; Silva et al., 2007). In addition, a Heat Pump can be solar, thus receiving energy from a sustainable source. This specific type of

Heat Pump provides high energy efficiency and is a trend that can be seen in the specialized literature, standing out by the application of a solar-type evaporator. This component is exposed to solar radiation and thus has a higher available thermal input in relation to a closed environment (without solar exposure). The Performance Coefficient (COP) of a Heat Pump with solar evaporator becomes higher in relation to the Heat Pump that makes use of other types of evaporators (Buker and Riffat, 2016; Omojaro and Breitkopf, 2013).

When aiming for a high performance solar Heat Pump, you need a favorable weather, with good solar incidence. This situation is widely explored in the scientific literature and encourages research for this type of water heating system. However, situations where solar Heat Pump operates without exposure to solar radiation should be analyzed, as rainy or cloudy days often occur in several regions. A solar collector with a solar evaporator can perform its function independently of the temporal conditions of the days, because it still has good efficiency if it has not been exposed to solar radiation (Willem et al., 2017; Li et al., 2007a; Li et al., 2007b). Willem et al. (2017) obtained a COP of 4 to 4.9 in winter and 7 to 9 in summer for a water heating Heat Pump operating with CO2. Li et al. (2007a) and Li et al. (2007b) obtained an average seasonal COP of 5.25.

The primary component for the high performance of a solar Heat Pump is its evaporator. Analyzing the energy plots that interact with this component allows to predict if the system will have good thermal performance. The thermal changes that happen with the solar evaporator are: solar radiation, ambient radiation, sensitive heat from the air, latent heat from the air and convection caused by wind. A research conducted by Scarpa and Tagliafico (2016) with a solar Heat Pump operating with refrigerant R134a obtained COP of 5.8, besides bringing analytical and experimental results on the above-mentioned energy parcels, with emphasis on air vapor condensation, generally neglected when designing the solar evaporator, due to the scarce data in the literature. This specific aspect for the analysis of air vapor condensation is a rare line of research and there are few papers published in this direction. The authors obtained values ranging from 20 to 30% in the participation of latent heat in the total rate received by the solar evaporator, theoretical and experimental difference of 15% for the mass of condensate and 10 to 20% for the heat rate exchanged for the condensate.

Finally, one parameter that influences the correct sizing of the evaporator for the Heat Pump is the efficiency of this component. This efficiency tells how much of the available energy in the environment that arrives in the evaporator is absorbed by the refrigerant that passes inside it. Kong et al. (2011) obtained values in the range of 0.88 to 0.91, Li et al. (2007a) obtained values equal to 1.08 and Hawlader, Chou and Ullah (2001) obtained values varying in the range of 0.4 to 0.75.

The objective of this work is to make an energetic analysis of a solar evaporator of a prototype of air-water Heat Pump, operating with refrigerated fluid R134a, in a condition of absence of solar radiation. All the thermal exchange properties are analyzed from an experimental test results and by applying mathematical models available in the literature.

2. METODOLOGY

The components of the system used in the Heat Pump are presented below, including the instrumentation used in the experimental evaluation, and the equations used to determine various parameters of energy analysis of the evaporator and the thermal performance of the system.

2.1 Experimental approach

The Heat Pump operates according to the steam compression cycle. In this system, the fluid that composes the hot source is the water stored in a tank with a storage capacity of 200 liters and the cold source is the ambient air of a research laboratory outside the influence of solar radiation located in the city of Belo Horizonte. The system operates with the following heat exchangers: a solar evaporator and an immersion condenser (copper tube in serpentine format) inside the tank. The Heat Pump has a hermetically sealed reciprocating compressor (1/3 HP nominal power) and a thermostatic expansion valve type expansion device. The cooling circuit has been instrumented with Bourdon type gauges and K type thermocouples. Figure 1 presents the Heat Pump and the construction data of the solar evaporator. The thermal reservoir and the solar evaporator (103x160 cm) are shown.

A device for collecting condensed water from the plate has been developed. The condensed water is formed on both sides of the plate. On the front face, the condensed liquid flows and falls into the lower portion of the plate. However, on the back side there is constant dripping all over its extension (due to the inclination), forcing the implantation of a collection device, composed by a waxed canvas positioned below the plate so that the condensed water falls and drips to the inferior area of the plate. In the lower portion of the plate there is a gutter to store the condensed, which covers the entire width of the plate, ensuring that all the condensed that is formed is collected.

The solar evaporator was installed at a fixed angulation of 30º to perform the test and below it was installed a system to collect condensed water that is conducted and accumulated in a trough in the lower portion, as shown in Figure 2. The volume of condensed water generated was measured by a graduated cylinder. The plate temperature (evaporator) was recorded by a type K thermocouple positioned in its central region.

Parameter	*Value*
Internal tube diameter	$D_{int_{evap}} = 8.73\ mm$
External tube diameter	$D_{ext_{evap}} = 9.53\ mm$
Plate thickness	$\delta_{al} = 1.0\ mm$
Tube length (excluding bends)	$z = 16.0\ m$
Developed curve length	$z' = 1.28\ m$
Plate width	$w_{pl} = 1.03\ m$
Plate length	$L_{pl} = 1.60\ m$
Plate area	$A_{pl} = 1.65\ m^2$
Plate Emissivity	$\varepsilon = 0.95$

Figure 1: Heat Pump and construction data of the solar evaporator.
(A) Solar evaporator and (B) thermal water reservoir.

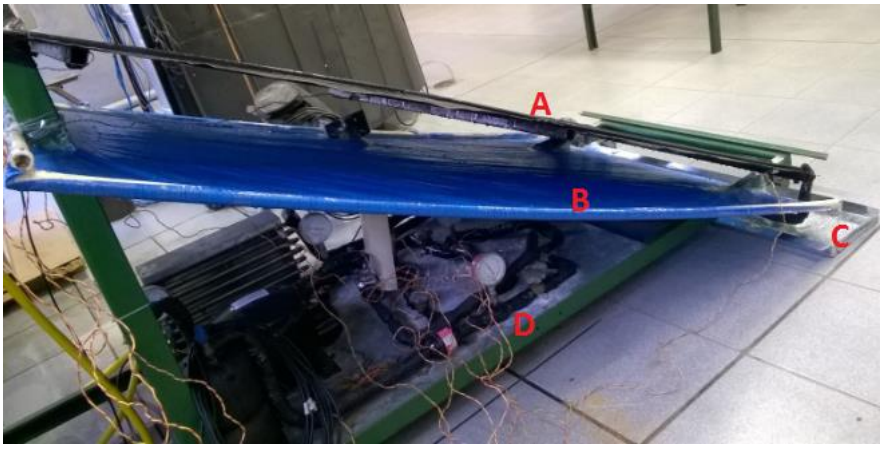

Figure 2: Side view of the Heat Pump. (A) Solar Evaporator, (B) Condensed fluid Collector System, (C) Condensed fluid Accumulator and (D) Cooling Cycle System.

Figure 3 presents the detail of the tank bottom with an internal view (where it is possible to notice the condenser by immersion) and constructive data of the component. A psychrometer was used to collect the ambient temperature and dew point data of the water vapor present in the air and an energy meter to monitor the real compressor energy consumption.

Parameter	Value
Internal tube diameter	8.73 mm
External tube diameter	9.53 mm
Tube length	4.5 m

Figure 3: Internal view of the tank where the condenser is located by immersion in serpentine format and constructive details of the component.

The water temperature in the tank was determined by averaging three points of stratified measurements in the tank (bottom, middle and top) by K-type thermocouples. The interval between the measurements of the quantities involved in the operation of the system was 15 minutes. The measured quantities were: temperatures and pressures of the thermodynamic steam compression cycle, water temperature, environment, plate and dew point temperature, the electrical energy consumed by the compressor and the generated volume of condensed water vapor.

In accordance with the manuals of the instruments (properly calibrated) used in this work, the measurement uncertainties were established in Table 1.

Table 1: Measurement inaccuracy of the used instruments.

Measuring instrument	Uncertainty
K-type Thermocouple	± 1 ºC
Bourdon pressure gauge (low pressure)	± 0.1 bar (1% of full scale)
Bourdon pressure gauge (high pressure)	± 0.35 kgf/cm² (1% of full scale)
Digital psychrometer	± 1 °C (ambient temperature) ± 2 °C (dew point temperature)
Energy meter	± 1%
Graduated Cylinder	± 2 ml
Tank	± 5%

2.2 Heat Pump thermal performance modelling process

The thermal performance of the heat pump was determined by Eq. (1), where m_w is the water mass, ΔT_w is the temperature variation of the water (final and initial state), c_{p_w} is the specific heat of the water at constant pressure, $\dot{W}_{\text{comp}}$ is the energy rate consumed by the compressor and t is the time between measurements.

$$COP = \frac{m_w c_{p_w} \Delta T_w}{\dot{W}_{comp} t} \tag{1}$$

It was considered that all the heat given off by the refrigerator $\dot{Q}_{cond}$ when passing through the condenser was fully absorbed by the water in the tank. Therefore, all the heat losses occurred by the tank were not considered. The rate of heat $\dot{Q}_{cond}$ is given by Eq. (2), where $h_{f_{cond_{out}}}$ and $h_{f_{cond_{in}}}$ are, respectively, the enthalpies of the refrigerant at the outlet and inlet of the condenser. In addition, $\dot{Q}_{cond}$ can be evaluated as the heating capacity of the system. Finally, $\dot{m}_f$ is the mass flow of refrigerant through the system.

$$\dot{Q}_{cond} = \dot{m}_f (h_{f_{cond_{in}}} - h_{f_{cond_{out}}}) \tag{2}$$

The ideal working rate of the compressor $\dot{W}_{comp_{ideal}}$ is given by Eq. (3), where $h_{f_{evap_{out}}}$ is the enthalpy of the refrigerant at the outlet of the evaporator.

$$\dot{W}_{comp_{ideal}} = \dot{m}_f (h_{f_{cond_{in}}} - h_{f_{evap_{out}}}) \tag{3}$$

The ideal working rate of the compressor considers only the thermodynamic cycle through the refrigerator. It does not take into account losses inside the compressor, such as heat losses to the outside environment and losses due to irreversibilities. The information of this parameter allows to determine the performance of the compressor η_{comp}, from Eq. (4).

$$\eta_{comp} = \frac{\dot{W}_{comp_{ideal}}}{\dot{W}_{comp}} \tag{4}$$

The test performed with the Heat Pump operating without the solar radiation (in the laboratory), i.e. simulating a rainy or cloudy day, indicated the formation of condensed water in the collector (solar evaporator). Therefore, the latent heat rate of the air, $q_{lat_{exp}}$, was considered. This value is based on experimental data, i.e. it is considered as real value, and not theoretical like the other values cited below. The contribution of the sensitive heat of the air q_{conv}, due to the natural convection of the air around the collector, and the radiation of the environment q_{rad} were also considered. That is, these three heat exchange parcels were responsible for the thermal contribution of the environment available to the collector when it is operated in the laboratory.

The efficiency of the collector η_{col}, given by Eq. (5), is assessed by the ratio of the heat rate absorbed by the refrigerant when passing the evaporator $\dot{Q}_{evap}$, given by Eq. (6), to the ambient heat rate arriving at the collector

$\dot{Q}_{evap_{ideal}}$, given by Eq. (7). Where $h_{f_{evap_{in}}}$ is the enthalpy of the refrigerant at the evaporator inlet. Furthermore, $\dot{Q}_{evap}$ can be evaluated as the energy absorption capacity of the environment by the refrigerant passing through the evaporator.

$$\eta_{col} = \frac{\dot{Q}_{evap}}{\dot{Q}_{evap_{ideal}}} \tag{5}$$

$$\dot{Q}_{evap} = \dot{m}_f (h_{f_{evap_{out}}} - h_{f_{evap_{in}}}) \tag{6}$$

$$\dot{Q}_{evap_{ideal}} = q_{lat_{exp}} + q_{rad} + q_{conv} \tag{7}$$

The η_{col} provides an important parameter for evaluating the energy performance of the collector, representing the percentage of the heat coming from the environment that is received by the collector and used by the refrigerator in its expansion when passing through the evaporator. Furthermore, it indicates how well sized the collector is for the system operating under certain conditions. The EES (Engineering Equation Solver) software was used to acquire all the properties of the fluids and solids described during the work.

2.3 Modelling procedures for heat exchange in the solar evaporator

The solar evaporator is a serpentine collector set (plate formed along the tube) built to take advantage of the natural or forced convection of the ambient air, by solar and ambient radiation, and by the latent condensation heat of water steam present in the air. This achieves a considerable increase in the heat exchange coefficient with the refrigerant.

In this prototype the solar evaporator is composed of a copper tube in serpentine shape fixed to a black painted aluminium plate to optimize the radiation absorption. Only the straight sections of the tube are on the plate, i.e. the curved sections are out of contact with the plate.

The solar evaporator is a kind of fin working with reverse direction of heat flow, i.e. the base receives heat instead of dissipating it. The tube remains cold by the refrigerant flow, acting as the base of the fin, and the portions of the plate serve as extended surfaces that conduct the heat captured from the environment to its base. Figure 4 (A) presents a dimensional scheme of the solar evaporator as a fin. Figure 5 (B) presents the segmentation of the evaporator into 10 fins, one next to the other. However, the mathematical equation treats as if they were all aligned, and not in parallel as it is manufactured for compacting reasons.

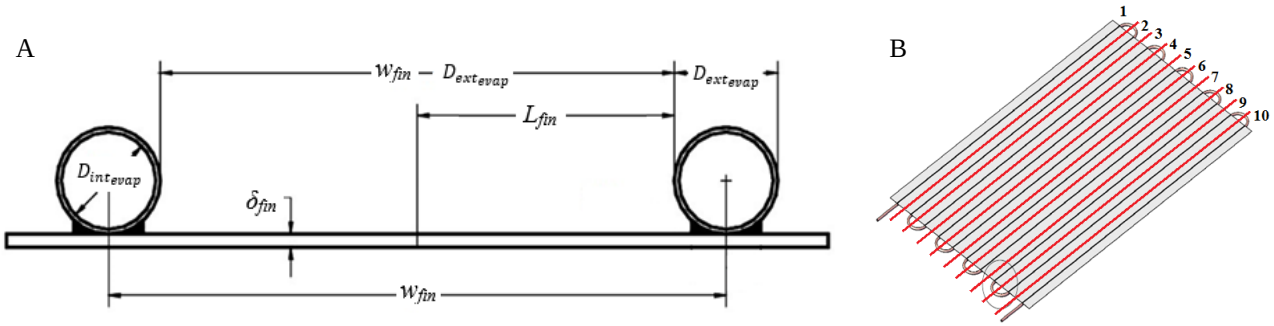

Figure 4: (A) Plate and tube dimensions. Source: Modified from Faria (2013), p. 96 and (B) Representation of plate and pipe segments. Modified from Reis (2012), p. 64.

The evaporator has 10 parallel tube segments joined to the plate and 9 bends out of contact with the plate. According to the data in Figure 1, the plate width is w_{pl} = 1030 mm, and then the characteristic fin width is $w_{fin} = w_{pl}/10$ = 103 mm. In addition, the characteristic fin length is $L_{fin} = (w_{fin} - D_{ext_{evap}})/2$ = 46.74 mm. Also δ_{fin} = 1 mm is the thickness of the fin. The depth of the page in Figure 4 represents the total length of the tube z = 16.0 m and the complete length of the fin. The tube dimensions are shown in Figure 1.

According to Incropera et al. (2007), the efficiency of the fin η_{al} should be determined in order to make possible the calculations of all the thermal changes that happen to it. The Eq. (8) allows the calculation of the perimeter P_{al} of the area exposed to heat flow through the fin, where δ_{al} is the thickness of the fin, the Eq. (9) allows the calculation of the cross section A_{cs} to heat flow through the fin and the Eq. (10) allows the calculation of the coefficient M of the fin.

$$P_{fin} = 2z + 2\delta_{fin} \tag{8}$$

$$A_{cs} = z\delta_{fin} \tag{9}$$

$$M = \sqrt{\frac{H_{ext}P_{fin}}{A_{cs}k_{fin}}} \tag{10}$$

Where H_{ext} is the external heat exchange coefficient to the fin, being the sum of the ambient radiation coefficient H_{rad} and the natural convection coefficient H_{conv}, according to Eq. (11), and k_{fin} is the thermal conductivity of the material that constitutes the fin.

$$H_{ext} = H_{conv} + H_{rad} \tag{11}$$

The area of one side of the A_{fin} fin is given by Eq. (12) and the area of the base of the A_b fin is given by Eq. (13). Finally, the efficiency of the fin can be determined by Eq. (14), which is responsible for determining how much of the fin area is actually used for heat exchange with the outside environment.

$$A_{fin} = 2zL_{fin} \tag{12}$$

$$A_b = \pi D_{ext_{evap}} z - 2\delta_{fin} z \tag{13}$$

$$\eta_{fin} = \frac{tanh(Mfin)}{ML_{fin}} \tag{14}$$

According to Incropera et al. (2007), the natural convection coefficient is given by Eq (15). In which L_{pl}=1600 mm is the length of the plate (collector) and plays the role of characteristic length.

$$H_{conv} = \frac{Nu_{conv}k_{air}}{L_{pl}} \tag{15}$$

Where k_{air} is the coefficient of thermal conductivity of the air at the average temperature between plate and air (film temperature) and Nu_{conv} is the Nusselt number for natural convection. The latter is given by Eq. (16).

$$Nu_{conv} = \left\{0{,}825 + \frac{0{,}387Ra^{1/6}}{\left[1+(0{,}492/Pr_{air})^{9/16}\right]^{8/27}}\right\}^2 \tag{16}$$

Where Pr_{air} is the Prandtl number of the air in the film temperature. Ra is the number of Rayleigh given by Eq. (17).

$$Ra = \frac{gcos\theta\beta(T_{air}-T_{pl})L_{pl}^3}{\alpha_{air}\upsilon_{air}} \tag{17}$$

Where g is the acceleration of gravity (9.81 m/s²), θ is the angle of inclination of the plate with the vertical (60º), β is the coefficient of thermal volumetric expansion (calculated by the inverse of the absolute temperature (Kelvin) of the film), T_{air} is the air temperature, T_{pl} is the average temperature of the plate, α_{air} is the thermal diffusivity of the air and υ_{air} is the kinematic viscosity of the air, the latter two being the temperature of the film. According to Incropera et al. (2007), the coefficient of ambient radiation is given by Eq (18).

$$H_{rad} = \varepsilon\sigma(T_{room} + T_{pl})(T_{room}^2 + T_{pl}^2) \tag{18}$$

Where σ is the Stefan-Boltzmann constant (5.67x10-8 W/m².k4) and T_{room} is the room temperature, considered equal to air temperature. The emissivity of the plate was determined by a field test using a thermographic camera. The resulting value was $\varepsilon = 0{,}95$. In addition, the plate was approximated to that of a gray body, i.e., the absorbtivity was considered the same as the emissivity.

Due to the relative humidity of the air, the water vapour present in the air suffers condensation on the surface of the plate, as it is at a temperature below the dew point. The dew point temperature T_{dp} is set based on local atmospheric pressure, relative air humidity (measured by a psychrometer) and ambient temperature (air) and is supplied by consultation with the EES.

Scarpa and Tagliafico (2016) used Eq. (19) in their research. This equation takes into account the dilution of water vapor in the atmospheric air. This approach consisted in calculating the mass transfer coefficient H_m for the condensation of a highly diluted system on a cold surface, based on the heat and mass transfer analogy, from the knowledge of the convective heat transfer coefficient at the air and plate interface.

$$H_m = \frac{H_{conv_{nat}}}{c_{p_{air}} \rho_{air} R_{a_v} T_{air}} \left(\frac{P_{air}}{P_v - P_{sat}}\right) In \left[\frac{P_{air} - P_{sat}}{P_{air} - P_v}\right] \quad (19)$$

Where $c_{p_{air}}$ is the specific heat at constant air pressure and ρ_{air} the specific air mass, both measured at room temperature. In addition, P_{air} is the atmospheric pressure, P_v is the partial vapour pressure in the air measured at the air temperature given by Eq. (20) and P_{sat} is the vapour saturation pressure measured at plate temperature. Finally, $R_{a_v} = 461{,}5\, J/kg.K$ is the gas constant of the water vapour. However, in Eq. (13), P_{sat} is evaluated at room temperature. Furthermore, ϕ is the relative humidity of the air.

$$P_v = \phi P_{sat} \quad (20)$$

The equations defining the coefficients of heat exchange by natural convection, ambient radiation and condensation are presented, which allow the calculation of the heat exchange rates of each of these energy parcels. These take into account the efficiency of the fin. It was also considered that the two faces of the plate exchange heat for ambient radiation, for natural convection and for condensation. In addition, the total tubular area of the bends was also considered, although small in relation to the plate area. The heat rate of ambient radiation q_{rad} exchanged by the evaporator and the vicinity is given by Eq. (21). In which the area of the bends A_{ben} (tubular area outside the plate) is given by Eq. (22), where z'=1.28 m is the developed length of the bends.

$$q_{rad} = H_{rad}(2\eta_{fin} A_{fin} + A_b + A_{ben})(T_{room} - T_{pl}) \quad (21)$$

$$A_{ben} = \pi D_{ext_{evap}} z' \quad (22)$$

Scarpa and Tagliafico (2016) used Eq. (23) for the calculation of the theoretical rate of heat by condensation of water vapour $q_{lat_{theoretical}}$ present in the air when condensing on the surface of the evaporator.

$$q_{lat_{theoretical}} = H_m(2A_{pl} + A_{ben})(P_v - P_{sat}) h_{lv_w} \quad (23)$$

Where h_{lv_w} is the enthalpy of the water vapour liquid measured in the dew temperature and $A_{pl} = 1{,}65\, m^2$ is the area of the plate. The natural convection heat rate q_{conv} is given by Eq. (24).

$$q_{conv} = H_{conv}(2\eta_{fin} A_{fin} + A_b + A_{ben})(T_{air} - T_{pl}) \quad (24)$$

The condensate was collected every 1 hour. The temperature of this water was already close to the ambient temperature, because the time that was stored in the gutter was enough for the thermal balance with the environment. Thus, it was possible to perform the experimental measurement of the condensate, performing a work similar to Scarpa and Tagliafico (2016), in which it served as a basis for comparison of results. Thus, the average mass flow of the experimental condensate $\dot{m}_{cond_{exp}}$ in the measurement range is given by Eq. (25).

$$\dot{m}_{cond_{exp}} = \frac{\rho_{cond} Vol_{cond}}{t} \quad (25)$$

Where ρ_{cond} is the specific mass of liquid water at room temperature and Vol_{cond} is the volume of water collected during the time period t. The theoretical mass flow of the condensate $\dot{m}_{cond_{theoretical}}$ can be calculated by Eq. (26). Where the modified liquid vapour water enthalpy h'_{lv_w} is given by Eq. (27).

$$\dot{m}_{cond_{theoretical}} = \frac{q_{lat_{theoretical}}}{h'_{lv_w}} \quad (26)$$

$$h'_{lv_w} = h_{lv_w} + 0{,}68 c_{p_{l_w}} (T_{dp} - T_{pl}) \quad (27)$$

Where $c_{p_{l_w}}$ is the specific heat at constant pressure of the saturated liquid water evaluated at the temperature of the film. Similarly, the average heat rate of condensation of experimental water vapour $q_{lat_{exp}}$ in the measurement range can be determined by Eq. (28).

$$q_{lat_{exp}} = \dot{m}_{cond_{exp}} . h'_{lv_w} \quad (28)$$

Theoretical and experimental values were compared, and the mean difference in values between them and how well the literature modeling describes the experimental situation were analyzed. Figure 5 shows the lower portion of the plate soaked with condensate, which is stored in the gutter.

Figure 5: Condensate storage in the gutter.

Finally, the contribution of the latent heat rate in relation to the total heat rate absorbed by the refrigerant x_{lat}, given by Eq. (29), is a scarce parameter in the literature and the target of this research.

$$x_{lat} = \frac{q_{lat_{exp}}}{\dot{Q}_{evap}} \tag{29}$$

2.4 Measurement Uncertainty

The methodology proposed by Taylor and Kuyatt (1994) was considered to be the most relevant way of evaluating the system for determining the spread of the COP uncertainty. Admitting the non-correlation and randomness between the uncertainties of the variables, the uncertainty of the calculated parameter can be given by Eq. (30).

$$u_Y = \sqrt{\sum_i \left(\frac{\partial Y}{\partial X_i}\right)^2 u_{X_i}^2} \tag{30}$$

Where u_Y is the uncertainty of the parameter calculated regarding the i uncertainty of u_{X_i} of the i variable X_i. The i partial derivation of the variable $\frac{\partial Y}{\partial X_i}$ makes it possible to determine its percentage contribution to the total uncertainty of the calculated parameter. The EES software was used to perform the uncertainty calculations.

3. RESULTS AND DISCUSSIONS

A heating test of 200 litres of water was carried out via a heat pump operating with the solar evaporator and immersion condenser. The water was heated from a temperature of 32.8 to 44.9 °C. The average ambient temperature was 28.2 °C and the average plate temperature was 10 °C. In addition, the average test time was 3h45min and 16 measurements of the variables were performed.

The average coefficient of performance of Heat Pump was 2.31±0.12. Figure 6 (A) shows the COP as a function of water heating temperature. The thermal performance of the system suffered degradation over time, ranging from 2.40 to 1.88. The compressor performance oscillated around an average value of 0.55. The average power consumed by the compressor was 325 W, from 308 to 344 W, as shown in Figure 6 (B). There was a continuous increase in the power consumed by the compressor with the evolution of the water heating process, which contributed to the degradation of the thermal performance of the system.

The efficiencies of the fin and the collector oscillated, respectively, around an average value of 0.95 and 0.88. The fin efficiency is relatively high, contributing positively to the collector efficiency. This efficiency is in accordance with the values found by Kong et al. (2011). This indicates the good sizing of the collector for the system when it operates in a null solar radiation situation. It is important to point out that this type of collector has a noticeably higher yield than the thermal solar collectors (which do not exceed 80%), because in the case of the solar evaporator, the working fluid is a frigorific fluid that flows at low temperatures (below 10 ºC), and it rejects little energy that comes from the environment.

The contribution of the heat rate provided by water vapor condensation (experimental) x_{lat} oscillated around an average value of 23% of the total. It should be noted that the modeling for the latent heat calculation resulted in mean values of 23% lower than those found experimentally. These results are in accordance with Scarpa and Tagliafico (2016).

The average contribution of the ambient radiation rate $q_{rad}/\dot{Q}_{evap}$ was 58%, representing the major source of heat exchange with the evaporator. Finally, the average contribution of the natural convection rate $q_{conv}/\dot{Q}_{evap}$ represented 30% of the total, being the second largest source of thermal exchange. It should be noted that when making the sum of

the three percentages already presented, they exceed 100%. This is due to the fact that the collector presents a yield of 88% and part of the energy that arrives there is not absorbed. Figure 7 (A) presents the heat exchange rates for radiation (average value of 327 W), convection (average value of 174 W) and experimental latent heat (average value of 133 W). The rates of radiation and convection are overestimated, as these actual rates are influenced by the efficiency of the collector.

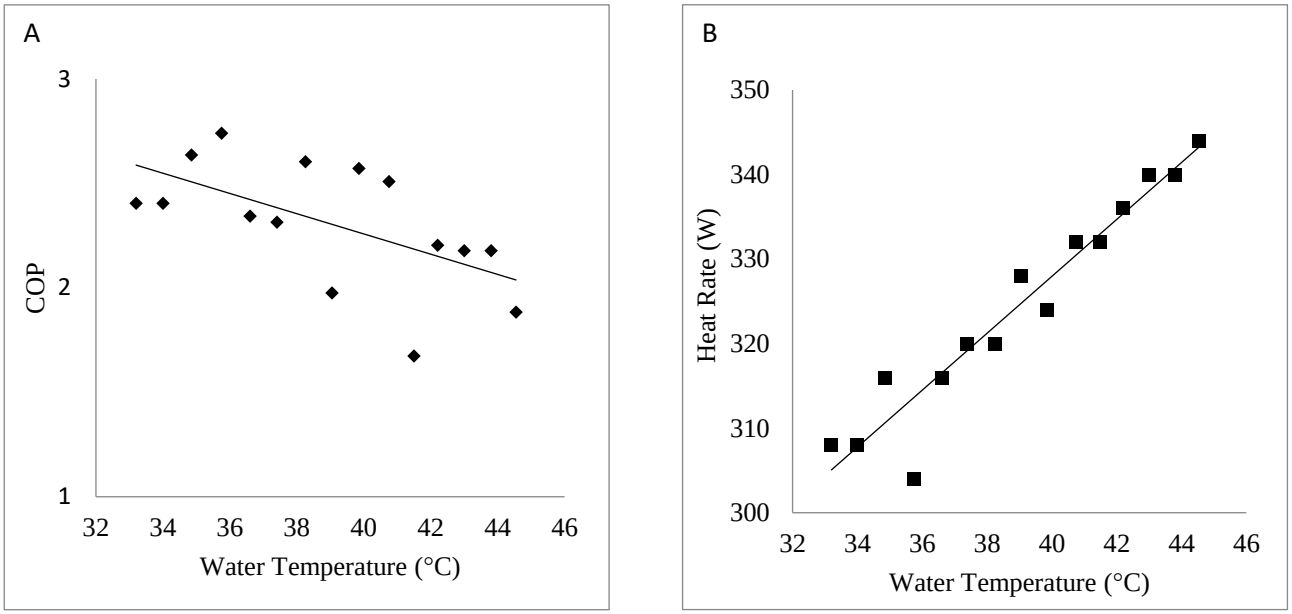

Figure 6: (A) COP as a function of water heating temperature. (B) Power consumed by the compressor.

Figure 7 (B) shows the behavior of condensate formation on the collector along the water heating. The values found experimentally were, on average, 25% higher than those estimated by the equations in the literature. This difference was higher than that found by Scarpa and Tagliafico (2016).

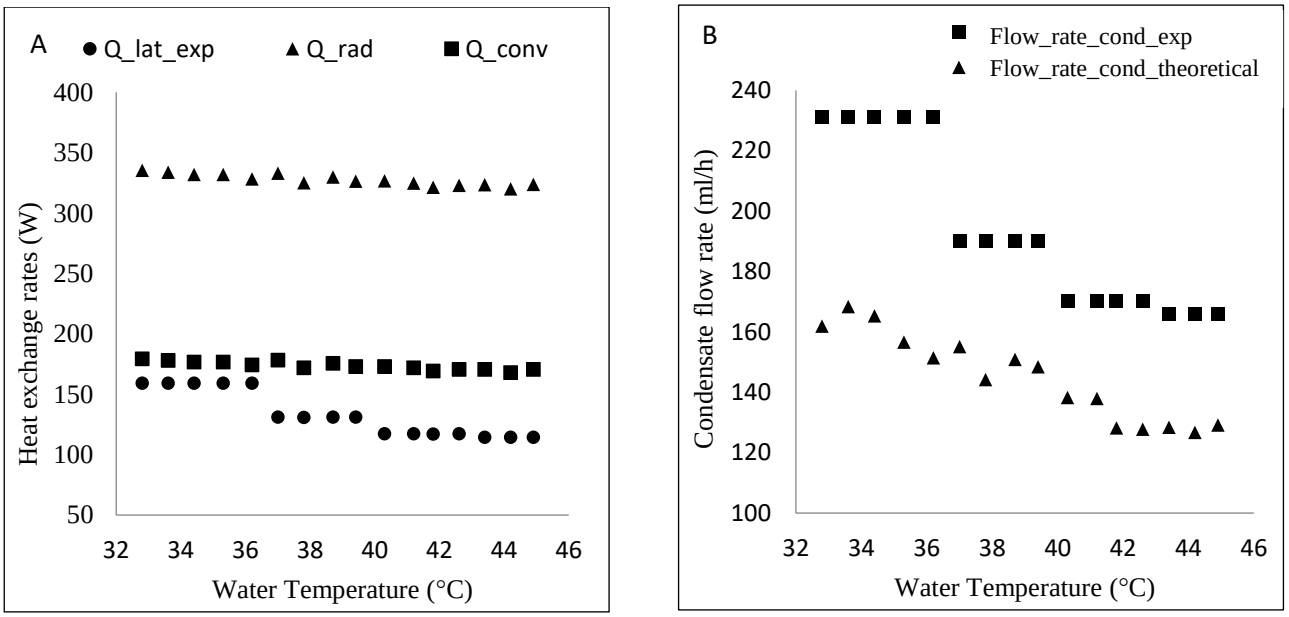

Figure 7: (A) Heat exchange rates for radiation, convection and latent heat. (B) Behavior of condensate formation on the collector throughout the system operation.

The difference between the theoretical and experimental value for condensate formation is directly related to the time frame of the condensate collection. The time range of one hour was relatively long and allowed to predict, in an experimental way, the average latent heat rate and the average condensate volume in this period, observed in the steps of Figure 7, while the theoretical value was able to predict this magnitude in a time range 75% lower (15 min). The experimental mean value was 193 ml/h and the theoretical value was 145 ml/h.

Finally, the heat rate of the environment $\dot{Q}_{evap_{real}}$ oscillated around 568 W and the average heating capacity of the system $\dot{Q}_{cond}$ oscillated around 747 W.

4. CONCLUSIONS

This work enabled the energy analysis of a solar evaporator and the thermal performance of a Heat Pump operating in a non-existent solar energy situation. It reflects conditions of cloudy or rainy days, in which the solar thermal input is negligible and the solar evaporator has only the energy present in the environment.

The heating of 200 litres of water from 32.8 to 44.9 °C took place in a time interval of 3.75 hours. The Heat Pump had an average heating capacity of 747 W and thermal performance of 2.31±0.12. The collector was well dimensioned for the environmental conditions, presenting an efficiency of 88%. The real contribution of the latent heat rate of the air in relation to the total rate exchanged with the solar evaporator was 23%, with an average deviation of 23% in relation to the value estimated by the equations in the literature. For the mass of condensate formed, this average deviation was 25%. The contribution of the heat rate by ambient radiation was higher than the others (more than 50%), followed by the convection rate and finally, the latent heat rate.

The results of this research reinforce the advantages of using a water heating system via a solar heat pump even when operating with an evaporator outside of exposure to solar radiation. The system proved to be very advantageous compared to traditional residential water heating equipment in Brazil (electric shower) that has, at most, COP equal to 1.

5. ACKNOWLEDGEMENTS

This work was supported by Foundation for Research Support of the State of Minas Gerais (FAPEMIG), National Council for Scientific and Technological Development (CNPq) and Coordination of Improvement of Higher Level Personnel (CAPES).

6. REFERÊNCIAS

Buker, M.S. and Riffat, S.B., 2016. “Solar assisted heat pump systems for low temperature water heating applications: A systematic review”. Renewable and Sustainable Energy Reviews, Vol. 55, p. 399-413.

EPE - Empresa de Pesquisa Energética, 2016a. “Eficiência Energética e Geração Distribuída para os próximos 10 anos (2015-2024)”, Rio de Janeiro, Brasil.

EPE - Empresa de Pesquisa Energética, 2016b. “BEM: Balanço Energético Nacional de 2016”, Rio de Janeiro, Brasil.

Faria, R.N., 2013. *Projeto e construção de uma bomba de calor a CO_2 operando em ciclo transcrítico e modelagem dinâmica do conjunto evaporador solar-válvula de expansão*. Ph.D. thesis, Post-Graduate Program in Mechanical Engineering, Federal University of Minas Gerais, Belo Horizonte.

Hawlader, M.N.A.; Chou, S.K. and Ullah, M.Z., 2001. “The performance of a solar assisted heat pump water heating system”. Applied Thermal Engineering, Vol. 21, p. 1049-1065.

Incropera, F.P., Dewitt, D.P., Bergman, T.L. and Lavine, A.S., 2007. Fundamentals of Heat and Mass Transfer. John Wiley and Sons, Hoboken, 6th edition.

Kong, X.Q., Zhang, D., Li, Y. and Yang, Q.M., 2011. “Thermal performance analysis of a direct-expansion solar-assisted heat pump water heater”. Energy, Vol. 36, p. 6830-6838.

Li, Y.W., Wang, R.Z., Wu, J.Y. and Xu, Y.X., 2007a. “Experimental performance analysis on a direct-expansion solar-assisted heat pump water heater” Applied Thermal Engineering, Vol. 27, p. 2858-2868.

Li, Y.W., Wang, R.Z., Wu, J.Y. and Xu, Y.X., 2007b. “Experimental performance analysis and optimization of a direct expansion solar-assisted heat pump water heater”. Energy, Vol. 32, p. 1361-1374.

Omojaro, P. and Breitkopf, C., 2013. “Direct expansion solar assisted heat pumps: A review of applications and recent research”. Renewable and Sustainable Energy Reviews, Vol. 22, p. 33-45.

Reis, R.V.M, 2012. *Análise experimental comparativa entre uma bomba de calor e uma resistência elétrica como dispositivo de apoio de energia para um aquecedor solar de água*. Ph.D. thesis, Post-Graduate Program in Mechanical Engineering, Federal University of Minas Gerais, Belo Horizonte.

Rodríguez, O.R.S., Koury, R.N.N. and Maia, A.A.T., 2015. “Socio-economic performance of a solar flat plate collector based in a heat pump water heating system in the brazilian southeast region”. International Congress of Mechanical Engineering – COBEM. Rio de Janeiro, Brasil.

Scarpa, F. and Tagliafico, L.A., 2016. “Exploitation of humid air latent heat by means of solar assisted heat pumps operating below the dew point”. Applied Thermal Engineering, vol. 100, p. 820-828.

Silva, I.C., Oliveira, R.N., Koury, R.N.N. and Machado, L., 2007. “Análise da viabilidade econômica e estudo do desempenho de uma bomba de calor ar-água como apoio ao sistema de coletor solar.” Congresso Iberoamericano de Engenharia Mecânica. Cusco, Peru.

Taylor B.N. and Kuyatt, C.E., 1994. “Guidelines for evaluating and expressing the uncertainty of NIST measurement results”. National Institute of Standards and Technology, technical note 1297.

Willem, H., Lin, Y. and Lekov, A., 2017. “Review of energy efficiency and system performance of residential heat pump water heaters”. Energy and Buildings, Vol. 143, p. 191-201.

7. RESPONSIBILITY NOTICE

The authors are the only responsible for the printed material included in this paper.